Triangle-Comparison Approach and Space Vector Approach to Pulsewidth Modulation in Inverter fed Drives

G.Narayanan **V.T.Ranganathan***
email: prjpmsm@ee.iisc.ernet.in vtran@ee.iisc.ernet.in
Department of Electrical Engg., Indian Institute of Science, Bangalore - 560 012, INDIA
Ph : 91 - 80 - 3600566
Fax : 91 - 80 - 3600444

Abstract :

This paper investigates the equivalence of the two popular approaches to Pulsewidth Modulation (PWM) in induction motor drives, namely the triangle-comparison approach and the space vector approach. It brings out the conditions wherein they are equivalent, and wherein they are not. It shows that the space vector approach is more general, and offers more degrees of freedom, compared to the triangle-comparison approach. Even a limited exploitation of these flexibilities has been reported to have improved the drive performance significantly. This gives adequate motivation to exploit these flexibilities further.

Triangle-Comparison Approach and Space Vector Approach to Pulsewidth Modulation in Inverter fed Drives

Abstract :

This paper investigates the equivalence of the two popular approaches to Pulsewidth Modulation (PWM) in induction motor drives, namely the triangle-comparison approach and the space vector approach. It brings out the conditions wherein they are equivalent, and wherein they are not. It shows that the space vector approach is more general, and offers more degrees of freedom, compared to the triangle-comparison approach. Even a limited exploitation of these flexibilities has been reported to have improved the drive performance significantly. This gives adequate motivation to exploit these flexibilities further.

1. Introduction :

In real-time Pulsewidth Modulation (PWM) techniques [1-10] like sine-triangle PWM [1] and conventional space vector modulation [2], a fundamental cycle is divided into several subcycles. The 3-phase voltages to be applied on the motor are specified in every subcycle, and are met in an average sense. Thus, a volt-second balance is maintained over every subcycle.

There are two popular approaches to real-time PWM, namely the triangle comparison approach and the space vector approach.

In the triangle-comparison approach, 3-phase modulating waves are compared against a common triangular carrier to determine the switching instants of the three phases. The modulating wave of a given phase specifies the duty ratio or the average pole voltage corresponding to that phase. Switching the phase at an appropriate instant ensures that the required average pole voltage over the given half-carrier cycle is met. The most common and

popular modulating waves are sinusoidal waves [1]. Any triplen frequency component can be added as zero sequence component to the 3-phase sinusoidal waves. Different triplen frequency components thus lead to different modulating waves with different spectral properties. The choice of these triplen frequency components is a degree of freedom in this approach [4-7].

A Voltage Source Inverter is shown in Fig.1. It has eight switching states. The voltage vectors corresponding to these eight states are as shown in Fig.2. In the space vector approach, the voltage reference is provided in terms of a revolving space vector. The magnitude and the frequency of the fundamental component are specified by the magnitude and frequency respectively of the reference vector. The reference vector is sampled once in every subcycle. The inverter is maintained in different states for appropriate durations such that an average voltage vector equal to the sampled reference vector is generated over the given subcycle. The inverter states used are the two zero states, and the two active states, whose voltage vectors are the closest to the commanded voltage vector. For a commanded vector in sector I, the states 0, 1, 2 and 7 can be used. To generate this vector in an average sense, the durations for which the active state 1, the active state 2, and the two zero states together must be applied are given by T_1, T_2 and T_Z respectively in Eq.(1).

$$T_1 = V_{REF}\sin(60^o-\alpha)/\sin(60^o), \quad T_2 = V_{REF}\sin(\alpha)/\sin(60^o), \quad T_Z = T_S - T_1 - T_2 \qquad \ldots (1)$$

The division of the duration T_Z between the two zero states 0 and 7 is a degree of freedom in the space vector approach. This division of T_Z in a subcycle is equivalent to adding a common-mode component to the 3-phase average pole voltages. Over a fundamental cycle, this is equivalent to the addition of triplen frequency components to the fundamental sinusoidal waves in the triangle-comparison approach [4-6]. That is, the same PWM waveform can be generated based on both the approaches. Hence, it has been concluded in the literature [4-6]

that the two approaches are equivalent. This equivalence has been exploited to make the implementation easier, both when the voltage reference is available as 3-phase sinusoidal modulating waves [7] or as a voltage vector [8].

This paper investigates the equivalence of the two approaches in greater detail, and in the light of newer PWM techniques reported [9,10]. That is, it studies whether the same PWM waveforms, generated based on the space vector approach, can be generated using the triangle-comparison approach as well. It brings out the conditions wherein such an equivalence does not exist, and establishes that the space vector approach is more general than the triangle-comparison approach.

2. Analysis at a subcycle level :

Several space vector-based PWM techniques have been reported [2,3,8-12]. It is to be studied whether the PWM waveforms generated by every one of these techniques can be generated using the triangle-comparison approach as well. A fundamental cycle is divided into several subcycles in real-time PWM as mentioned earlier. Hence, the equivalence can first be studied at the subcycle level.

Different switching sequences can be used to generate a given average vector in the space vector approach. For the same average vector, different switching sequences result in different sets of switching instants of the three phases. It is studied whether the same switching instants can be determined based on the triangle-comparison approach as well.

2.1 Switching sequences :

Given an average vector in sector I, the states that can be used are 0, 1, 2 and 7. Both the zero states can be used to generate the given average vector using sequences 0127 or

7210. These are termed as 'Type-I sequences' here. The total zero state duration is divided equally between the two zero states in conventional space vector modulation, while it is divided unequally in modified space vector modulation [11,12]. Alternatively, only one zero state can be used to generate the given average vector. Thus, sequences 012, 210, 721 or 127 can be used to generate the given average vector in sector I. These involve only two switchings instead of three. Such sequences are termed as 'Type-II sequences' in this paper.

It can be seen that the active state 1 can as well be applied over more than one interval, all falling within the given subcycle and adding up to T_1, to generate the given average vector. This applies to the active state 2 as well. Hence, sequences like 0121, 1210, 7212 or 2127, where an active state time is divided into two equal halves, can also be used to generate the given average vector [9-11]. These sequences are termed as 'Type-III sequences' here.

All the above three types of sequences can be used to generate any arbitrary average vector. An arbitrary vector needs both the active vectors. However, an average vector along a sector boundary needs only one active vector. For a vector on the boundary between sectors VI and I, the active vector 1 alone is needed. Hence sequence 010 or 101 can be used to generate such an average vector [9,10]. These are termed as 'Type-IV sequences' here.

2.1.1 Type-I sequences :

The pole voltages and the line voltages, normalised with respect to $0.5V_{DC}$, over the given subcycle are as shown in Figs.3a and 3b for sequences 0127 and 7210 respectively. All the three phases switch once within the subcycle. The duty ratios of the three phases in the given subcycle depend on V_{REF} and α as shown below :

$d_R = (T_1 + T_2 + T_7)/T_S = 0.5 + 0.5*V_{REF}*\cos(30^o-\alpha)/\sin(60^o)$

$d_Y = (T_2 + T_7)/T_S = 0.5 + V_{REF}*\sin(\alpha-30^o)$

$$d_B = T_7 / T_S = 0.5 - 0.5*V_{REF}*\cos(30^o-\alpha)/\sin(60^o) \quad \text{... (2)}$$

The average values of the 3-phase pole voltages over the given subcycle are also shown in dashed lines in Fig.3 along with the respective pole voltages. The expressions for the average pole voltages, normalised with respect to $0.5V_{DC}$, for the three phases are :

$$m_R = 2(d_R-0.5) = V_{REF}*\cos(30^o-\alpha)/\sin(60^o)$$

$$m_Y = 2(d_Y-0.5) = 2*V_{REF}*\sin(\alpha-30^o)$$

$$m_B = 2(d_B-0.5) = - V_{REF}*\cos(30^o-\alpha)/\sin(60^o) \quad \text{... (3)}$$

It can be seen that the sum of the three average pole voltages is not zero, implying the presence of a common-mode component. The mean value of these three average pole voltages is the common-mode component. Average pole voltage minus the common-mode component is the component that actually drives the motor currents. This component is termed as the 'sinusoidal component' of the average pole voltage in this paper.

The common-mode component over the given subcycle is :

$$m_C = (m_R + m_Y + m_B)/3 = 2*V_{REF}*\sin(\alpha-30^o)/3 \quad \text{... (4)}$$

The sinusoidal components of the 3-phase average pole voltages over the given subcycle are :

$$m_{SR} = V_{REF}*\cos(30^o-\alpha)/\sin(60^o) - 2*V_{REF}*\sin(\alpha-30^o)/3$$

$$m_{SY} = 4*V_{REF}*\sin(\alpha-30^o)/3$$

$$m_{SB} = - V_{REF}*\cos(30^o-\alpha)/\sin(60^o) - 2*V_{REF}*\sin(\alpha-30^o)/3 \quad \text{... (5)}$$

Thus, $m_C = 0.5*m_{SY}$ ... (6)

Thus, when a Type-I sequence is used to generate the given average vector, the common-mode component is half the sinusoidal component of the phase that switches between the two active states in the given sector.

Comparing the average pole voltages with a falling ramp as shown in Fig.3a gives the same switching instants of the individual phases as with the sequence 0127. In case of sequence 7210, the ramp is a rising one as shown in Fig.3b. Thus, when Type-I sequences are used, the same switching instants can be determined using the triangle-comparison approach as well. In other words, Type-I sequences have equivalence in the triangle-comparison approach.

2.1.2 Type-II sequences :

Sequences 012, 210, 721 and 127 can be used for generating a sample in sector I. The switching states, pole voltages and line voltages over a subcycle are shown in Fig.4 for sequences 012 and 210, and in Fig.5 for sequences 721 and 127.

Sequences 012 and 210 :

When a Type-II sequence using the zero state 0, namely 012 or 210, is used for generating an arbitrary average vector in sector I, the duty ratios of the three phases in the given subcycle are as follows :

$d_R = (T_1 + T_2)/ T_S = V_{REF}*\cos(30^o-\alpha)/\sin(60^o)$

$d_Y = T_2 / T_S = V_{REF}*\sin(\alpha)/\sin(60^o)$

$d_B = 0$ ... (7)

The average pole voltages, normalised with respect to $0.5V_{DC}$, of the three phases over the given subcycle are as follows :

$$m_R = 2(d_R-0.5) = 2*V_{REF}*\cos(30^o-\alpha)/\sin(60^o) - 1$$

$$m_Y = 2(d_Y-0.5) = 2*V_{REF}*\sin(\alpha)/\sin(60^o) - 1$$

$$m_B = 2(d_B-0.5) = - 1 \qquad \text{... (8)}$$

The common-mode component and the sinusoidal components of the three phases are as follows :

$$m_C = (m_R + m_Y + m_B)/3$$

$$= (2/3)*V_{REF}*\cos(30^o-\alpha)/\sin(60^o) + (2/3)*V_{REF}*\sin(\alpha)/\sin(60^o) - 1 \qquad \text{... (9)}$$

$$m_{SR} = (4/3)*V_{REF}*\cos(30^o-\alpha)/\sin(60^o) - (2/3)*V_{REF}*\sin(\alpha)/\sin(60^o)$$

$$m_{SY} = -(2/3)*V_{REF}*\cos(30^o-\alpha)/\sin(60^o) + (4/3)*V_{REF}*\sin(\alpha)/\sin(60^o)$$

$$m_{SB} = -(2/3)*V_{REF}*\cos(30^o-\alpha)/\sin(60^o) - (2/3)*V_{REF}*\sin(\alpha-30^o)/\sin(60^o) \qquad \text{... (10)}$$

Hence, $m_C = -1 - m_{SB}$ ... (11)

Thus, the common-mode component is related to the sinusoidal component of the phase which is clamped during the given subcycle, and can be derived from this component.

Sequences 721 and 127 :

When a Type-II sequence using the zero state 7, namely 721 or 127, is used for generating an arbitrary average vector in sector I, the duty ratios of the three phases in the given subcycle are as follows :

$d_R = 1$

$d_Y = (T_7 + T_2)/ T_S = 1 - V_{REF}*\sin(60^o-\alpha)/\sin(60^o)$

$d_B = T_7 / T_S = 1 - V_{REF}*\cos(30^o-\alpha)/\sin(60^o)$ ... (12)

The average pole voltages, normalised with respect to $0.5V_{DC}$, and the common-mode component of the average pole voltages are as follows :

$m_R = 2(d_R-0.5) = 1$

$m_Y = 2(d_Y-0.5) = 1 - 2*V_{REF}*\sin(60^o-\alpha)/\sin(60^o)$

$m_B = 2(d_B-0.5) = 1 - 2*V_{REF}*\cos(30^o-\alpha)/\sin(60^o)$ ... (13)

$m_C = (m_R + m_Y + m_B)/3$

$= 1 - (2/3)*V_{REF}*\sin(60^o-\alpha)/\sin(60^o) - (2/3)*V_{REF}*\cos(30^o-\alpha)/\sin(60^o)$ ... (14)

The sinusoidal components of the average pole voltages of the three phases are :

$m_{SR} = (2/3)*V_{REF}*\sin(60^o-\alpha)/\sin(60^o) + (2/3)*V_{REF}*\cos(30^o-\alpha)/\sin(60^o)$

$m_{SY} = -(4/3)*V_{REF}*\sin(60^o-\alpha)/\sin(60^o) + (2/3)*V_{REF}*\cos(30^o-\alpha)/\sin(60^o)$

$m_{SB} = (2/3)*V_{REF}*\sin(60^o-\alpha)/\sin(60^o) - (4/3)*V_{REF}*\cos(30^o-\alpha)/\sin(60^o)$ ... (15)

Hence, $m_C = 1-m_{SR}$ ... (16)

Thus, the common-mode component is related to the sinusoidal component of the phase which is clamped during the given subcycle as earlier.

The average pole voltages for the three phases over the given subcycle are shown in Figs.5 and 6. Comparing these average pole voltages with ramps as shown in the figures gives the switching instants of the individual phases. The ramps are falling ones in case of sequences 012 and 127, while they are rising ones in case of sequences 721 and 210. Thus, Type-II sequences also have equivalence in the triangle-comparison approach.

2.1.3 Type-III sequences :

Switching sequence 0121, 1210, 7212 or 2127 can also be used to generate an arbitrary average vector in sector I. The switching states, pole voltages and line voltages over a subcycle are shown for all these four sequences in Figs.6 and 7.

The duty ratios and the average pole voltages of three phases in case of sequences 0121 and 1210 are identical to those in case of sequences 012 and 210. Similarly, the duty ratios and the average pole voltages in case of 7212 and 2127 are identical to those in case of 721 and 127. Hence, the expressions given in section 2.1.2 are valid for Type-III sequences as well.

The average pole voltages of the three phases over the given subcycle while generating the given commanded vector are shown in Figs.6 and 7. The Y-phase switches twice within the subcycle. Hence, the switching instants of this phase cannot be determined by comparing its average pole voltage with a ramp as in the earlier cases. Thus, there is no equivalence for Type-III sequences in the triangle-comparison approach.

If the switching instants of the Y-phase are to be determined using its average pole voltage, then the signal used for comparison must be an 'asymmetric double-ramp' (instead of

a ramp) as shown in dashed and dotted lines in Figs.6 and 7. The two ramps, which constitute this signal, have different slopes. They divide the subcycle into two unequal durations, namely T_a and T_b, as shown. Their relative slopes change with change in the average pole voltage. The average pole voltage varies with both V_{REF} and α. Thus, the signal required for comparison is dependent on both V_{REF} and α.

In addition, the asymmetric double-ramp signal cannot be used for the other phase that switches. For this phase, the comparison of the average pole voltage must be done with a ramp as in the case of Type-I and Type-II sequences. Thus, the signals to be used for comparison are different for different phases.

The implications of the above are that the three phases cannot have a common carrier, and the carrier waveshape itself is dependent on the modulation index.

2.1.4 Type-IV sequences :

Switching sequences 010 and 101 can be used to generate an average vector on the boundary between sectors VI and I. The states, pole voltages and line voltages within the subcycle are shown in Fig.8. The duty ratios and the average pole voltages of the three phases over the subcycle are as shown below :

$$d_R = V_{REF}$$

$$d_Y = 0$$

$$d_B = 0 \qquad \text{... (17)}$$

$$m_R = 2(d_R-0.5) = 2*V_{REF} - 1$$

$$m_Y = 2(d_Y-0.5) = -1$$

$$m_B = 2(d_B-0.5) = -1 \qquad \text{... (18)}$$

The average common-mode component is as shown below :

$$m_C = (m_R + m_Y + m_B)/3 = (2/3)*V_{REF} - 1 \quad \text{... (19)}$$

The sinusoidal components of the 3-phase average pole voltages are :

$$m_{SR} = (4/3)*V_{REF}$$

$$m_{SY} = -(2/3)*V_{REF}$$

$$m_{SB} = -(2/3)*V_{REF} \quad \text{... (20)}$$

Hence, $m_C = -1 - m_{SY} = -1 - m_{SB}$ ... (21)

Thus, the common-mode component is related to the sinusoidal components of the two phases that are clamped over the subcycle.

One phase switches twice, while the other two remain clamped over the given subcycle. The switching instants of the double-switching phase cannot be determined by comparing its average pole voltage with a ramp signal. Thus, there is no equivalence in the triangle-comparison approach for Type-IV sequences also, as is the case with Type-III sequences.

If the switching instants of the double-switching phase are to be determined using its average pole voltage, then its average pole voltage must be compared against a 'double-ramp' signal (instead of a ramp) as shown in Fig.10. This signal is symmetric unlike the one in case of Type-III sequences. Also, the shape of this signal does not vary with modulation index. Hence, the carrier waveshape is independent of the modulation index. This same signal can be used for the other two phases also. Hence, the three phases can have a common carrier.

The study was carried out at a subcycle level in this section. It will be done at a fundamental cycle level in the following section using some PWM strategies as example cases.

3. Equivalent modulating and carrier waves :

Some space vector-based synchronised PWM strategies have been presented recently [9,10]. Of these strategies, the Conventional Space Vector Strategy (CSVS) uses only the Type-I sequences; the Basic Bus Clamping Strategy (BBCS) uses Type-I and Type-II sequences; the Asymmetric Zero-Changing Strategy (AZCS) uses Type-II and Type-III sequences; and the Boundary Sampling Strategy (BSS) uses Type-I, Type-II and Type-IV sequences.

The modulation process involved in any space vector-based technique can be seen in terms of equivalent modulating waves and equivalent carrier waves, the comparison of which results in the same PWM waveforms as generated by the given technique. The equivalent modulating and carrier waves corresponding to these strategies are presented in this section. It is shown that the equivalent carrier waves are triangular waves only in case of CSVS and BBCS. In case of AZCS and BSS, which use Type-III and Type-IV sequences respectively, the equivalent carrier is not a regular, isosceles triangular wave. Instead it is irregular and/or discontinuous.

3.1 Conventional Space Vector Strategy (CSVS) :

The modulating wave in the triangle-comparison approach is nothing but the variation of the average pole voltage over a fundamental cycle. The variation of the average pole voltage and its two components over a fundamental cycle in case of the conventional space vector strategy can be determined based on the expressions derived in section 2.1.1. These

average pole voltage waveforms are the equivalent modulating waves, which change with the modulation index.

In conventional space vector strategy with the number of samples per sector N=3 [9,10], the sequences used during the three subcycles in sector I are 0127, 7210 and 0127 respectively. Alternatively, sequences 7210, 0127 and 7210 respectively can also be used for the three samples. The former can be referred to as case (i), while the latter can be referred to as case (ii).

The average pole voltage for a given V_{REF} is the same for both cases. This waveform corresponding to V_{REF} = 0.866 is shown in both Figs.9a and 9b in dashed lines. PWM patterns, identical to the ones produced by case (i), can be generated by comparing the average pole voltage wave with a triangular carrier wave as shown in Fig.9a. This carrier has a positive zero-crossing at the positive zero-crossing of the modulating sinusoidal component. Comparison of the same average pole voltage waveform with a triangular carrier as shown in Fig.9b leads to PWM waveforms identical to the ones that can be generated by case(ii). This carrier wave has a negative zero-crossing at the positive zero-crossing of the modulating sinusoidal component, which is the preferred case in synchronised sine-triangle PWM.

3.2 Basic Bus Clamping Strategy (BBCS) :

Based on the expressions derived in sections 2.1.1 and 2.1.2, the average pole voltage and its two components corresponding to BBCS can be calculated. The variation of the average pole voltage of a phase over a fundamental cycle corresponding to BBCS with N=5 is shown in Fig.10 for V_{REF} = 0.866. Depending on the choice of switching sequences used, BBCS with N=5 produces two types of PWM waveforms, namely 60^o clamping and 30^o clamping waveforms. In the former, every phase is clamped during the middle 60^o duration of

every half cycle of its fundamental. In the latter, every phase remains clamped during the middle 30^o duration of every quarter cycle of its fundamental [9,10]. The variation of the average pole voltage corresponding to 60^o clamping and 30^o clamping are shown in Figs.10a and 10b respectively. These average pole voltage waveforms are the equivalent modulating waves corresponding to the different cases considered.

The equivalent carrier waves can be constructed using the ramp signals, discussed in sections 2.1.1 and 2.1.2. The equivalent carrier waves are triangular carrier waves once again as in the case of the conventional space vector strategy and are shown in Fig.10.

In case of 60^o clamping, the carrier wave has a positive zero-crossing at the positive zero-crossing of the modulating sinusoidal component as in case (i) of the conventional space vector strategy. It may be noted that the sequence used for the middle sample of sector I is 7210 in both these cases.

In case of the 30^o clamping, the carrier wave has a negative zero-crossing at the positive zero-crossing of the modulating sinusoidal component as in case (ii) of the conventional space vector strategy. It may be noted that the sequence used for the middle sample of sector I is 0127 in both these cases.

Thus, the PWM patterns, identical to the ones generated by BBCS, can be generated by comparing these equivalent modulating and carrier waves. The nature of the common-mode components is different for the conventional space vector strategy, BBCS with 60^o clamping scheme and BBCS with 30^o clamping scheme. The equivalent carrier waves are the regular, isosceles triangular waves for both these strategies, which are the synchronised versions of the conventional and the modified forms of space vector modulation, discussed in the literature [11,12]. Such a study is carried out in the following sections for two other synchronised PWM strategies.

3.3 Asymmetric Zero-Changing Strategy (AZCS) :

The equivalent modulating and carrier waves corresponding to AZCS with N=6 and 60^o clamping are as shown in Fig.11a, while those corresponding to AZCS with N=6 and 30^o clamping are as shown in Fig.11b, both for V_{REF}=0.866. It can be seen that the equivalent carrier waves are discontinuous at 60^o, 120^o, 240^o and 300^o. The asymmetric double-ramp can be seen in the subcycles ending with 180^o and 360^o. Thus, the equivalent carrier waves are irregular, and have a periodicity equal to the fundamental period.

The equivalent carrier waves corresponding to AZCS with N=6 and 30^o clamping scheme for the same V_{REF} are shown in Figs.12a, 12b and 12c for R-, Y- and B-phases respectively. It can be seen that the carrier waves are different for the three phases.

3.4 Boundary Sampling Strategy (BSS) :

The average pole voltage waveforms corresponding to BSS with N=4 and N=6 are presented in Figs.13a and 13b respectively for V_{REF}=0.866. The corresponding equivalent carrier waves are also shown in Figs.13a and 13b respectively. Symmetric double-ramp can be seen in the subcycles, where Type-IV sequences are used. In case of N=4, the carrier is discontinuous at the start and end of such subcycles. The periodicity of the equivalent carrier waves is one third of the fundamental period.

In the triangle-comparison, the number of half-carrier cycles per 180^o must be odd for Half Wave Symmetry, and must be even per 120^o for 3-Phase Symmetry. Hence, the number of half-carrier cycles per 60^o must be odd. On the other hand, the number of subcycles per sector can be either odd or even in the space vector approach.

3.5 Performance

The total harmonic distortion factor of the no-load current waveform (I_{THD}), or equivalently, the weighted total harmonic distortion factor of the line voltage waveform (V_{WTHD}) is a suitable performance measure for evaluating different PWM strategies.

$$I_{THD} = \sqrt{(\sum I_n^2)} / I_1 \quad , n \neq 1 \quad \text{... (22)}$$

$$V_{WTHD} = \sqrt{(\sum (V_n/n)^2)} / V_1 \quad , n \neq 1 \quad \text{... (23)}$$

where I_1 and I_n are the RMS values of the fundamental and nth harmonic currents respectively, and V_1 and V_n are the RMS values of the fundamental and nth harmonic voltages respectively.

Use of Type-III sequences leads to lesser current ripple at higher modulation indices than the use of Type-I sequences [11]. For a pulse number of 9, the computed V_{WTHD} vs. M characteristics are presented for CSVS, AZCS and BSS in Fig.14a. The corresponding measured I_{THD} vs. M characteristics are presented in Fig.14b. It can be seen that AZCS and BSS perform better than any other comparable strategy at different ranges of modulation indices. Thus, Type-III and Type-IV sequences help in improving the performance of motor drives significantly at middle and higher speed ranges.

4. Discussion

In Fig.3 the total zero state duration T_Z is equally divided between the zero states **0** and **7**. For the same T_Z if T_0 is decreased and T_7 increased, it can be seen that all the three average pole voltages increase. All the three increase by the same measure. That is, it is only their common-mode component that changes, and not the sinusoidal components. The relation between the ratio

of division of T_Z and the common-mode component has been brought out by Blasko [4]. Using this, the PWM waveforms generated by any triangle-comparison based PWM technique can be generated using the space vector approach as well. Similarly, the PWM waveforms generated by any space vector-based PWM technique, using Type-I and Type-II sequences alone, can be generated based on the triangle comparison approach also. Thus, when only Type-I and Type-II sequences are used, the space vector approach is equivalent to the triangle-comparison approach.

This equivalence has found use in simplifying PWM calculations. From Figs.4 to 6 it can be seen that given a set of 3-phase average pole voltages, the difference between the maximum one and the middle-valued one is a measure of one active state duration, and the difference between the middle-valued one and the minimum one is a measure of the other active state time. This is true for any set of 3-phase average pole voltages irrespective of their common-mode component. Thus, given a set of 3-phase sinusoidal modulating waves, the two active state durations can be arrived at from them, avoiding the trigonometric calculations given in Eq.(1). This has been exploited by Chung *et al* to simplify the calculations [7].

Because of this equivalence, many authors refer to the PWM techniques based on both the triangle-comparison approach and the space vector approach as 'carrier-based PWM' [5-6,11-12]. These two are viewed as only two approaches for calculations and implementation, and are referred to as 'triangle-intersection technique' and 'direct digital implementation' respectively [5-6].

However, when Type-III or Type-IV sequences are used, the two approaches are no longer equivalent. These sequences involve the application of a state more than once within a subcycle. This means switching of a phase more than once in the subcycle. However, switching of a phase more than once in a half-carrier cycle is not possible in the triangle-comparison

approach. Thus, the space vector approach is more general than the triangle-comparison approach.

5. Conclusion

The division of the total zero state duration between the two zero states is only one of the degrees of freedom available in the space vector approach. The space vector approach permits the use of different switching sequences to generate a given average vector over a subcycle. These sequences may involve the division of an active state time, switching of a phase more than once within the subcycle *etc.* Two such sequences were considered in this paper. It is shown that the PWM waveforms generated by space vector-based techniques, using such sequences, cannot be generated by comparing suitable 3-phase modulating waves against a common triangular carrier. That is, they have no equivalence in the triangle comparison approach.

More strategies are possible with such sequences. Type-III sequences involve double-switching of the phase that switches between the two active states. Sequences involving double-switching of either of the other two phases can also be considered. Sequences may involve more than three switchings per subcycle also. Thus, more such sequences are possible which exploit the flexibilities in the space vector approach. As the two strategies considered help improve the performance of the drives significantly at medium and higher speed ranges, there are adequate reasons to investigate PWM strategies using such new sequences.

References

1. A.Schonung and H.Stemmler, "Static frequency changers with subharmonic control in conjunction with reversible variable-speed AC drives", Brown Bov. Rev., Vol. 51, Aug./Sept. 1964, pp. 555-577.

2. H.W.van der Broeck, H.C.Skudelny and G.V.Stanke, "Analysis and realisation of a pulsewidth modulator based on voltage space vectors", IEEE Trans. IA, Vol. IA-24(1), 1988, pp. 142-150.

3. P.G.Handley and J.T.Boys, "Practical real-time PWM modulators- An assessment", IEE Proc.B, Vol. 139(2), 1992, pp.96-102.

4. V.Blasko, "Analysis of a hybrid PWM based on modified space-vector and triangle-comparison methods", IEEE Trans. IA-33(3), 1997, pp. 756-764.

5. A.M.Hava, R.J.Kerkman and T.A.Lipo, "A high performance generalised discontinuous PWM algorithm", IEEE Trans. IA, Vol. IA-34(5), 1998, pp. 1059-1071.

6. A.M.Hava, R.J.Kerkman and T.A.Lipo, "Simple analytical and graphical methods for carrier-based PWM-VSI drives", IEEE Trans. PE, Vol. PE-14(1), 1999, pp. 49-61.

7. Dae-Woong Chung, Joohn-Sheok Kim and Seung-Ki Sul, "Unified voltage modulation technique for real-time three-phase power conversion, IEEE Trans. IA, Vol. IA-34(2), 1998, pp. 374-380.

8. J-H.Youm and B-H.Kwon, "An effective software implementation of the space-vector modulation", Letter to the Editor, IEEE Trans. IE, Vol.IE-46(4), 1999, pp. 866-868.

9. G.Narayanan and V.T.Ranganathan, "Synchronised PWM strategies based on space vector approach. Part 1 : Principles of waveform generation", IEE Proc.B, Vol. 146(3), 1999, pp. 267-275.

of division of T_Z and the common-mode component has been brought out by Blasko [4]. Using this, the PWM waveforms generated by any triangle-comparison based PWM technique can be generated using the space vector approach as well. Similarly, the PWM waveforms generated by any space vector-based PWM technique, using Type-I and Type-II sequences alone, can be generated based on the triangle comparison approach also. Thus, when only Type-I and Type-II sequences are used, the space vector approach is equivalent to the triangle-comparison approach.

This equivalence has found use in simplifying PWM calculations. From Figs.4 to 6 it can be seen that given a set of 3-phase average pole voltages, the difference between the maximum one and the middle-valued one is a measure of one active state duration, and the difference between the middle-valued one and the minimum one is a measure of the other active state time. This is true for any set of 3-phase average pole voltages irrespective of their common-mode component. Thus, given a set of 3-phase sinusoidal modulating waves, the two active state durations can be arrived at from them, avoiding the trigonometric calculations given in Eq.(1). This has been exploited by Chung *et al* to simplify the calculations [7].

Because of this equivalence, many authors refer to the PWM techniques based on both the triangle-comparison approach and the space vector approach as 'carrier-based PWM' [5-6,11-12]. These two are viewed as only two approaches for calculations and implementation, and are referred to as 'triangle-intersection technique' and 'direct digital implementation' respectively [5-6].

However, when Type-III or Type-IV sequences are used, the two approaches are no longer equivalent. These sequences involve the application of a state more than once within a subcycle. This means switching of a phase more than once in the subcycle. However, switching of a phase more than once in a half-carrier cycle is not possible in the triangle-comparison

approach. Thus, the space vector approach is more general than the triangle-comparison approach.

5. Conclusion

The division of the total zero state duration between the two zero states is only one of the degrees of freedom available in the space vector approach. The space vector approach permits the use of different switching sequences to generate a given average vector over a subcycle. These sequences may involve the division of an active state time, switching of a phase more than once within the subcycle *etc.* Two such sequences were considered in this paper. It is shown that the PWM waveforms generated by space vector-based techniques, using such sequences, cannot be generated by comparing suitable 3-phase modulating waves against a common triangular carrier. That is, they have no equivalence in the triangle comparison approach.

More strategies are possible with such sequences. Type-III sequences involve double-switching of the phase that switches between the two active states. Sequences involving double-switching of either of the other two phases can also be considered. Sequences may involve more than three switchings per subcycle also. Thus, more such sequences are possible which exploit the flexibilities in the space vector approach. As the two strategies considered help improve the performance of the drives significantly at medium and higher speed ranges, there are adequate reasons to investigate PWM strategies using such new sequences.

References

1. A.Schonung and H.Stemmler, "Static frequency changers with subharmonic control in conjunction with reversible variable-speed AC drives", Brown Bov. Rev., Vol. 51, Aug./Sept. 1964, pp. 555-577.

2. H.W.van der Broeck, H.C.Skudelny and G.V.Stanke, "Analysis and realisation of a pulsewidth modulator based on voltage space vectors", IEEE Trans. IA, Vol. IA-24(1), 1988, pp. 142-150.

3. P.G.Handley and J.T.Boys, "Practical real-time PWM modulators- An assessment", IEE Proc.B, Vol. 139(2), 1992, pp.96-102.

4. V.Blasko, "Analysis of a hybrid PWM based on modified space-vector and triangle-comparison methods", IEEE Trans. IA-33(3), 1997, pp. 756-764.

5. A.M.Hava, R.J.Kerkman and T.A.Lipo, "A high performance generalised discontinuous PWM algorithm", IEEE Trans. IA, Vol. IA-34(5), 1998, pp. 1059-1071.

6. A.M.Hava, R.J.Kerkman and T.A.Lipo, "Simple analytical and graphical methods for carrier-based PWM-VSI drives", IEEE Trans. PE, Vol. PE-14(1), 1999, pp. 49-61.

7. Dae-Woong Chung, Joohn-Sheok Kim and Seung-Ki Sul, "Unified voltage modulation technique for real-time three-phase power conversion, IEEE Trans. IA, Vol. IA-34(2), 1998, pp. 374-380.

8. J-H.Youm and B-H.Kwon, "An effective software implementation of the space-vector modulation", Letter to the Editor, IEEE Trans. IE, Vol.IE-46(4), 1999, pp. 866-868.

9. G.Narayanan and V.T.Ranganathan, "Synchronised PWM strategies based on space vector approach. Part 1 : Principles of waveform generation", IEE Proc.B, Vol. 146(3), 1999, pp. 267-275.

References :

1. A.Schonung and H.Stemmler, "Static frequency changers with subharmonic control in conjunction with reversible variable-speed AC drives", Brown Bov. Rev., Vol. 51, Aug./Sept. 1964, pp. 555-577.

2. H.W.van der Broeck, H.C.Skudelny and G.V.Stanke, "Analysis and realisation of a pulsewidth modulator based on voltage space vectors", IEEE Trans. IA, Vol. IA-24(1), 1988, pp. 142-150.

3. P.G.Handley and J.T.Boys, "Practical real-time PWM modulators - An assessment", IEE Proc.B, Vol. 139(2), 1992, pp. 96-102.

4. V.Blasko, "Analysis of a hybrid PWM based on modified space-vector and triangle-comparison methods", IEEE Trans. IA-33(3), 1997, pp. 756-764.

5. A.M.Hava, R.J.Kerkman and T.A.Lipo, "A high performance generalised discontinuous PWM algorithm", IEEE Trans. IA, Vol. IA-34(5), 1998, pp. 1059-1071.

6. A.M.Hava, R.J.Kerkman and T.A.Lipo, "Simple analytical and graphical methods for carrier-based PWM-VSI drives", IEEE Trans. PE, Vol. PE-14(1), 1999, pp. 49-61.

7. Dae-Woong Chung, Joohn-Sheok Kim and Seung-Ki Sul, "Unified voltage modulation technique for real-time three-phase power conversion, IEEE Trans. IA, Vol. IA-34(2), 1998, pp. 374-380.

8. J-H.Youm and B-H.Kwon, "An effective software implementation of the space-vector modulation", Letter to the Editor, IEEE Trans. IE, Vol.IE-46(4), 1999, pp. 866-868.

9. G.Narayanan and V.T.Ranganathan, "Synchronised PWM strategies based on space vector approach. Part 1 : Principles of waveform generation", IEE Proc.B, Vol. 146(3), 1999, pp. 267-275.

10. __ , "Synchronised PWM strategies based on space vector approach. Part 2 : Performance assessment and application to V/f drives", IEE Proc.B, Vol. 146(3), 1999, pp. 276-281.

11. J.Holtz, "Pulsewidth modulation - a survey", IEEE Trans. IE, Vol. IE-39(5), 1992, pp. 410-420.

12. J.Holtz, "Pulsewidth modulation for electronic power conversion", Proc. IEEE, Vol. 82(8), 1994, pp. 1194-1214.

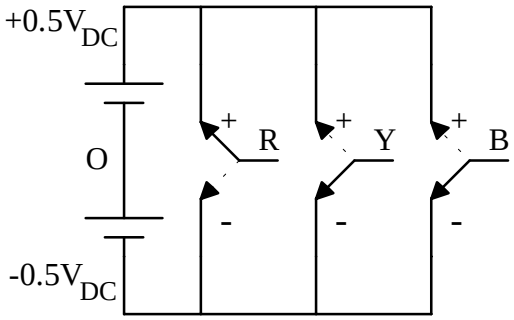

Fig. 1 Voltage Source Inverter

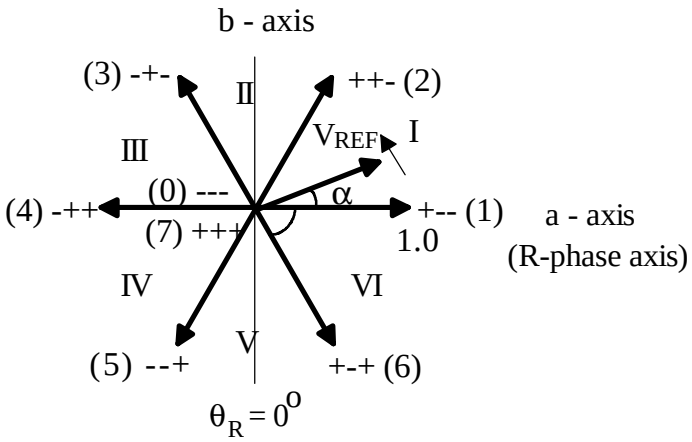

Fig. 2 Voltage space vectors produced by an inverter

θ_R = Angle of R-phase fundamental voltage

I, II, III, IV, V and VI : Sectors

Fig.3 Transitions in a subcycle - sequences 0127 and 7210

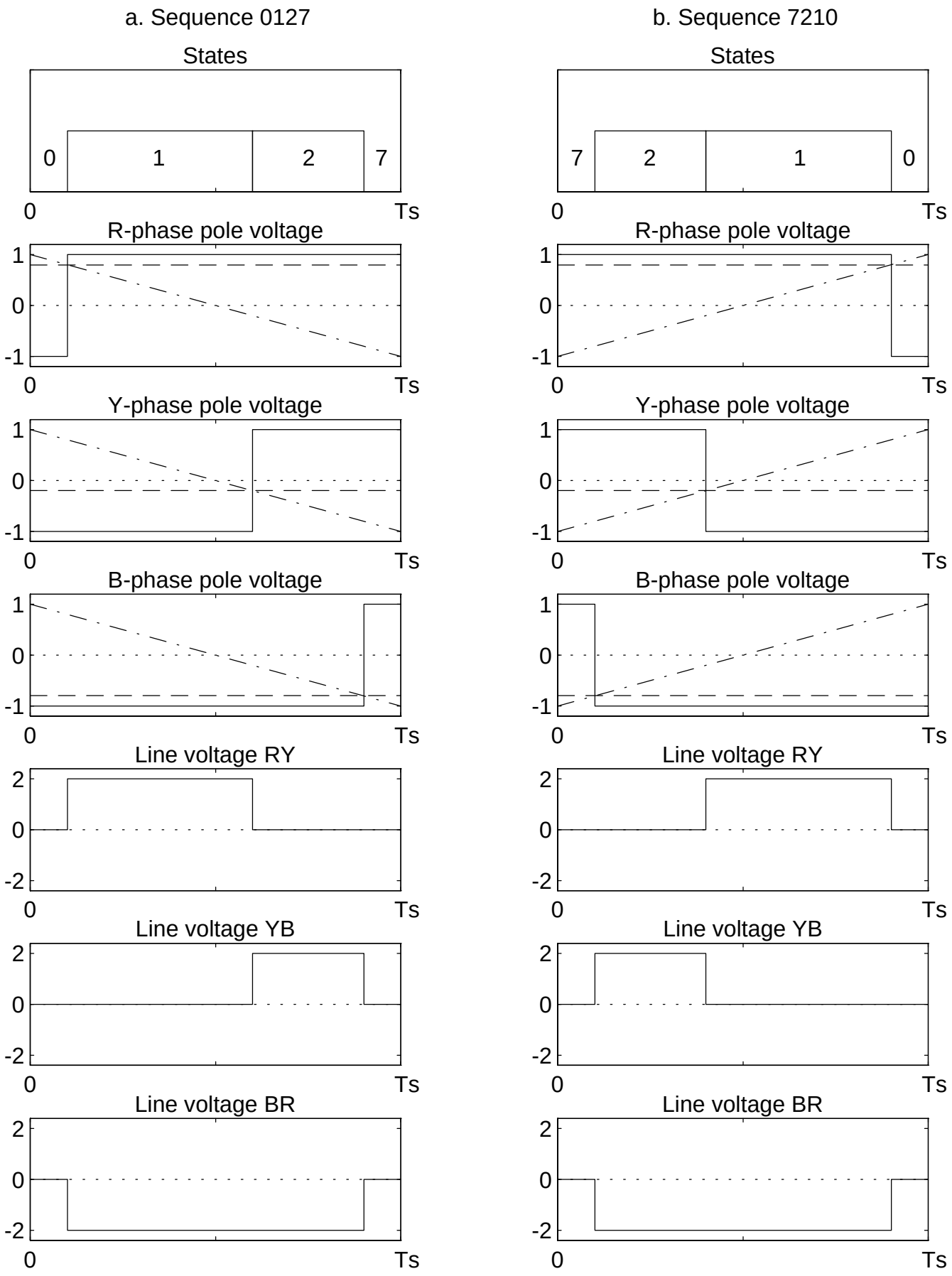

Fig.4 Transitions in a subcycle - sequences 012 and 210

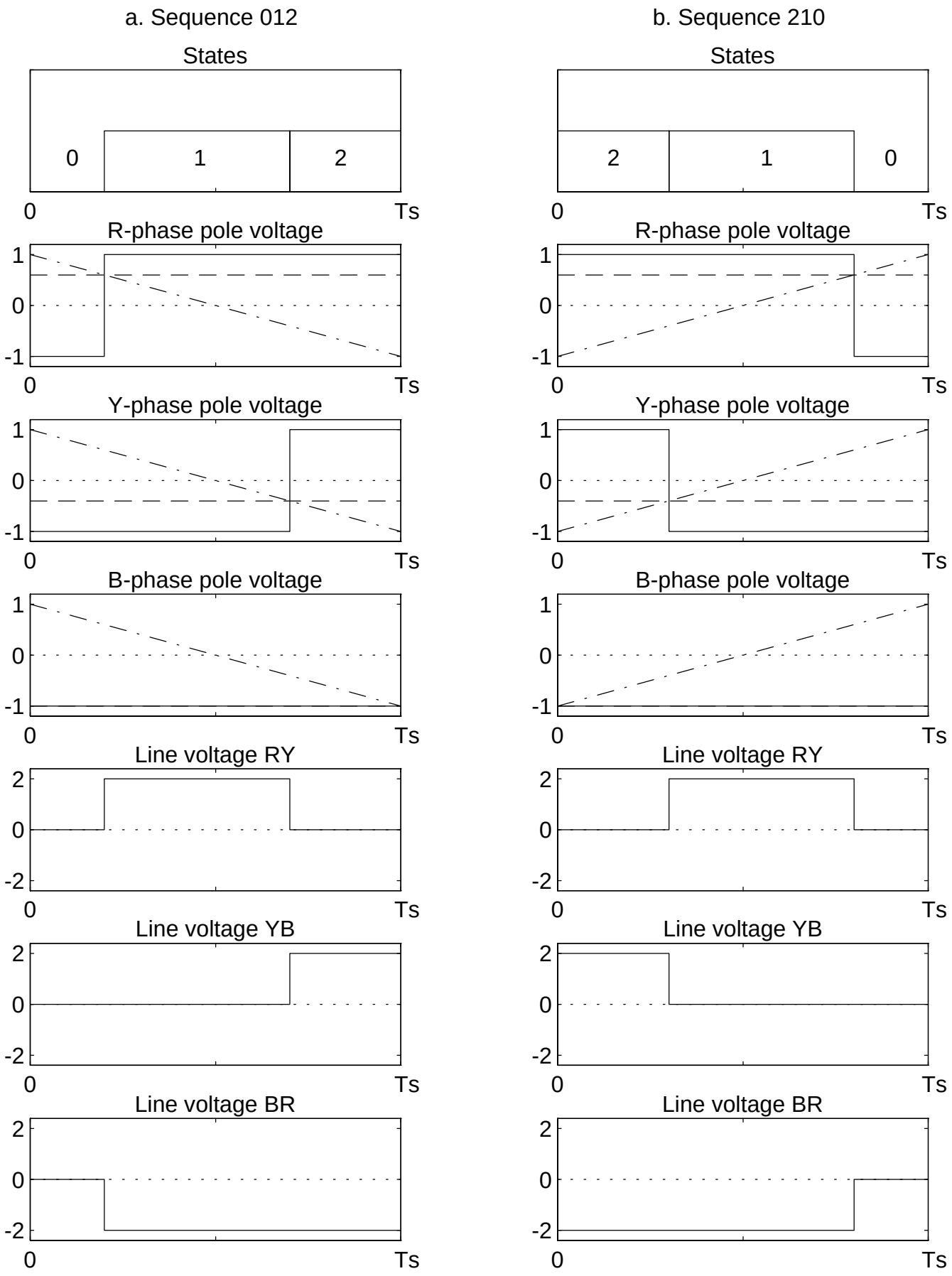

Fig.5 Transitions in a subcycle - sequences 721 and 127

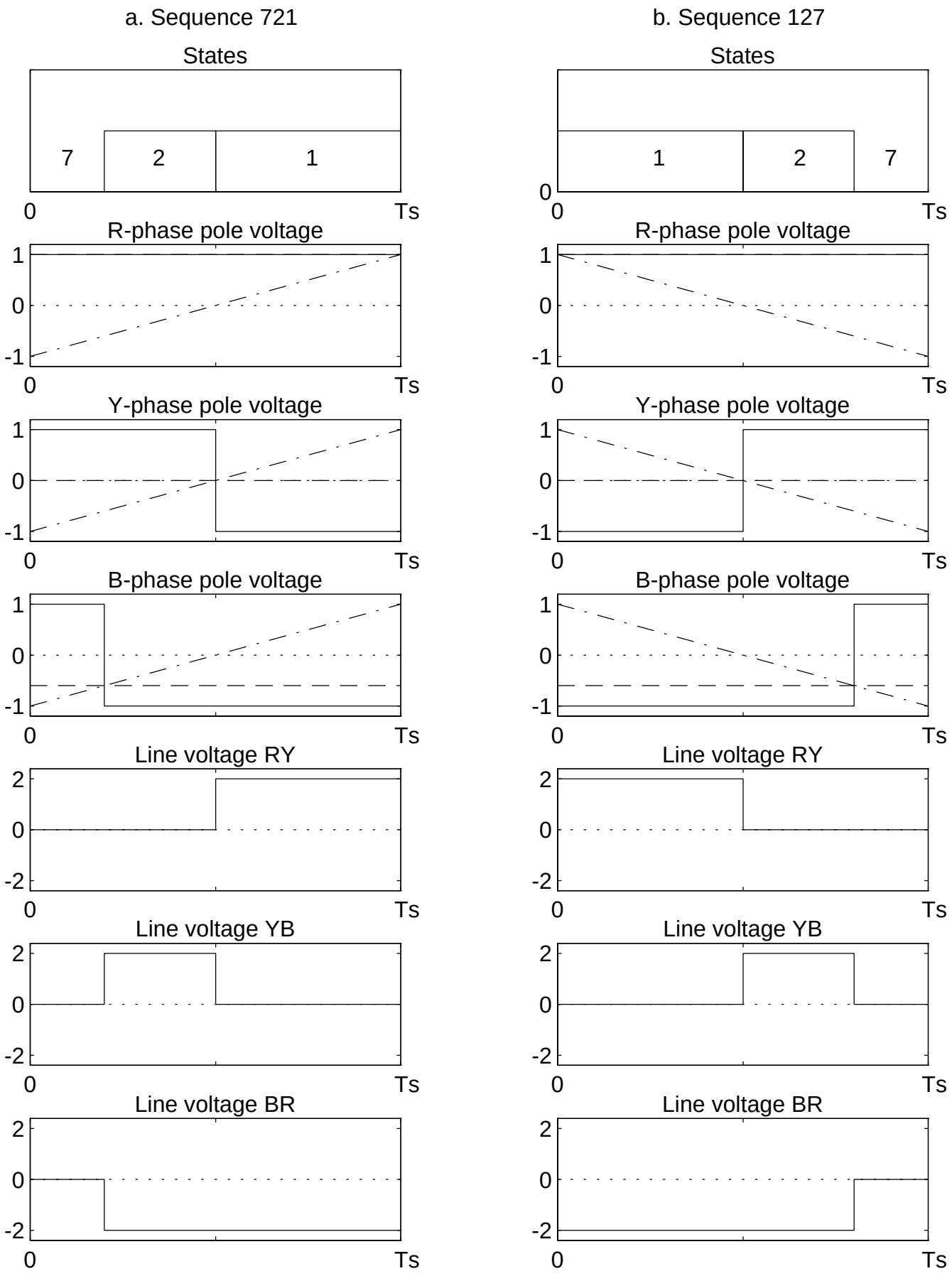

Fig.6 Transitions in a subcycle - sequences 0121 and 1210

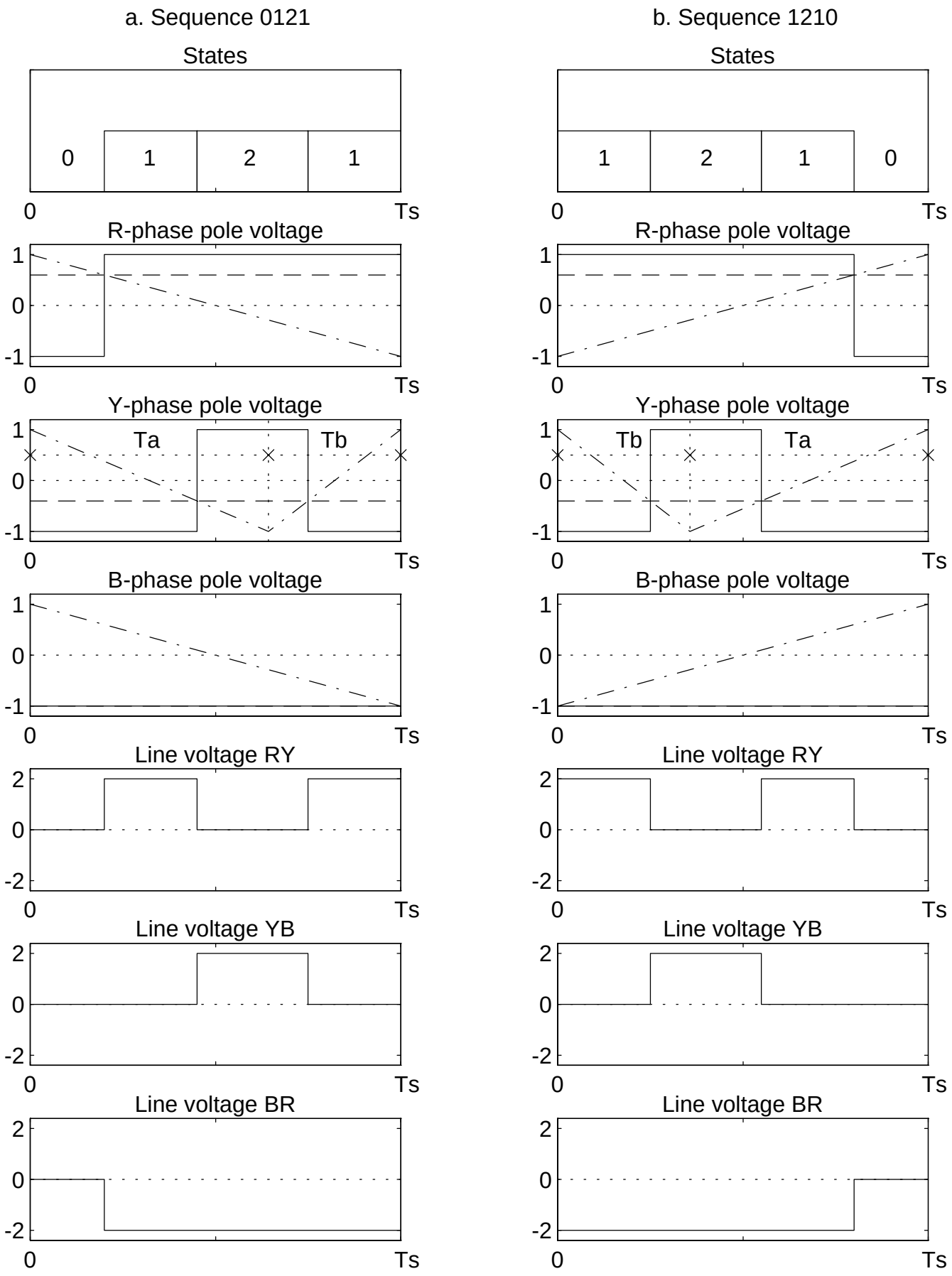

Fig.7 Transitions in a subcycle - sequences 7212 and 2127

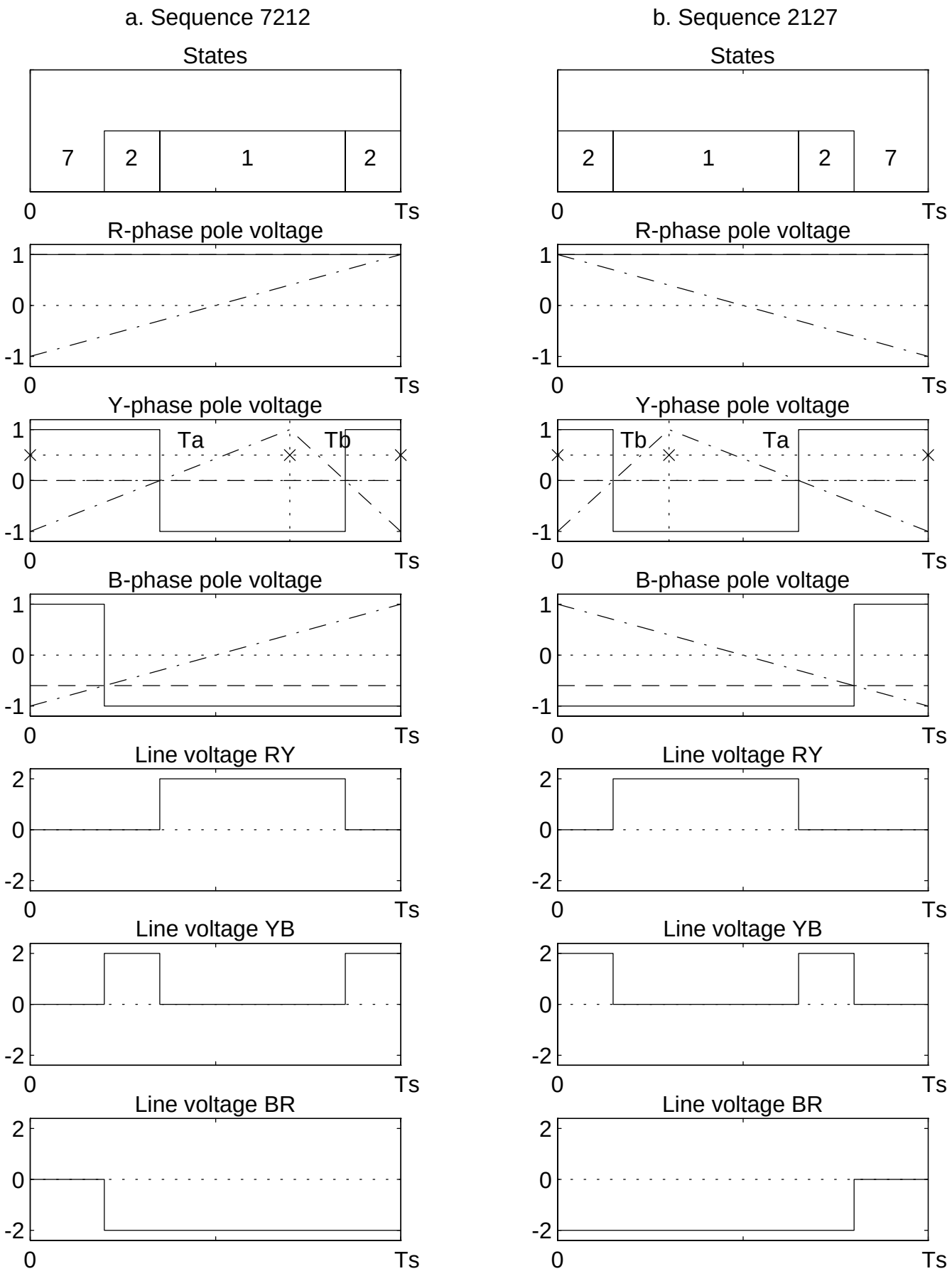

Fig.8 Transitions in a subcycle - sequences 010 and 101

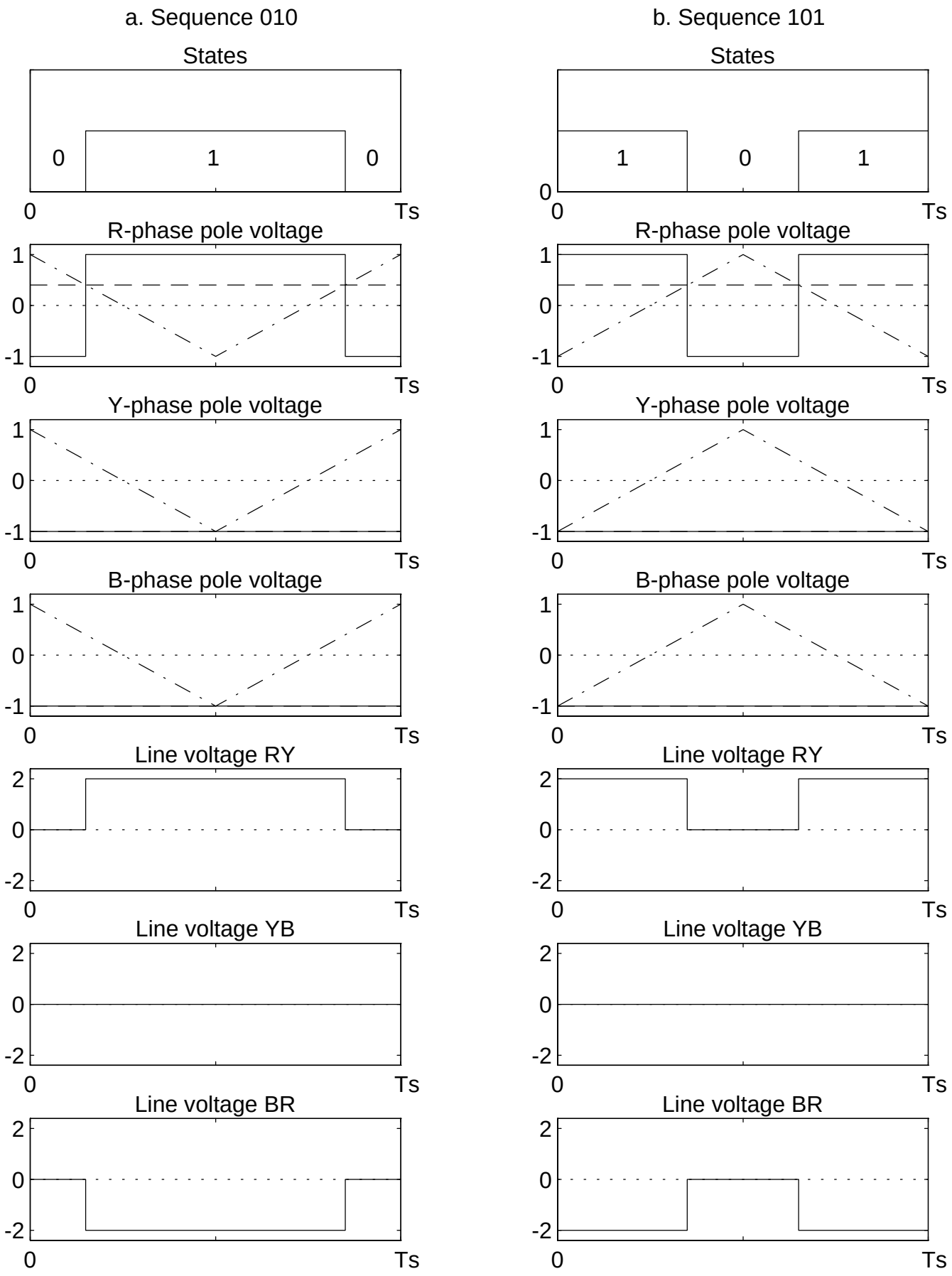

Fig.9 Equivalent modulating and carrier waves - CSVS

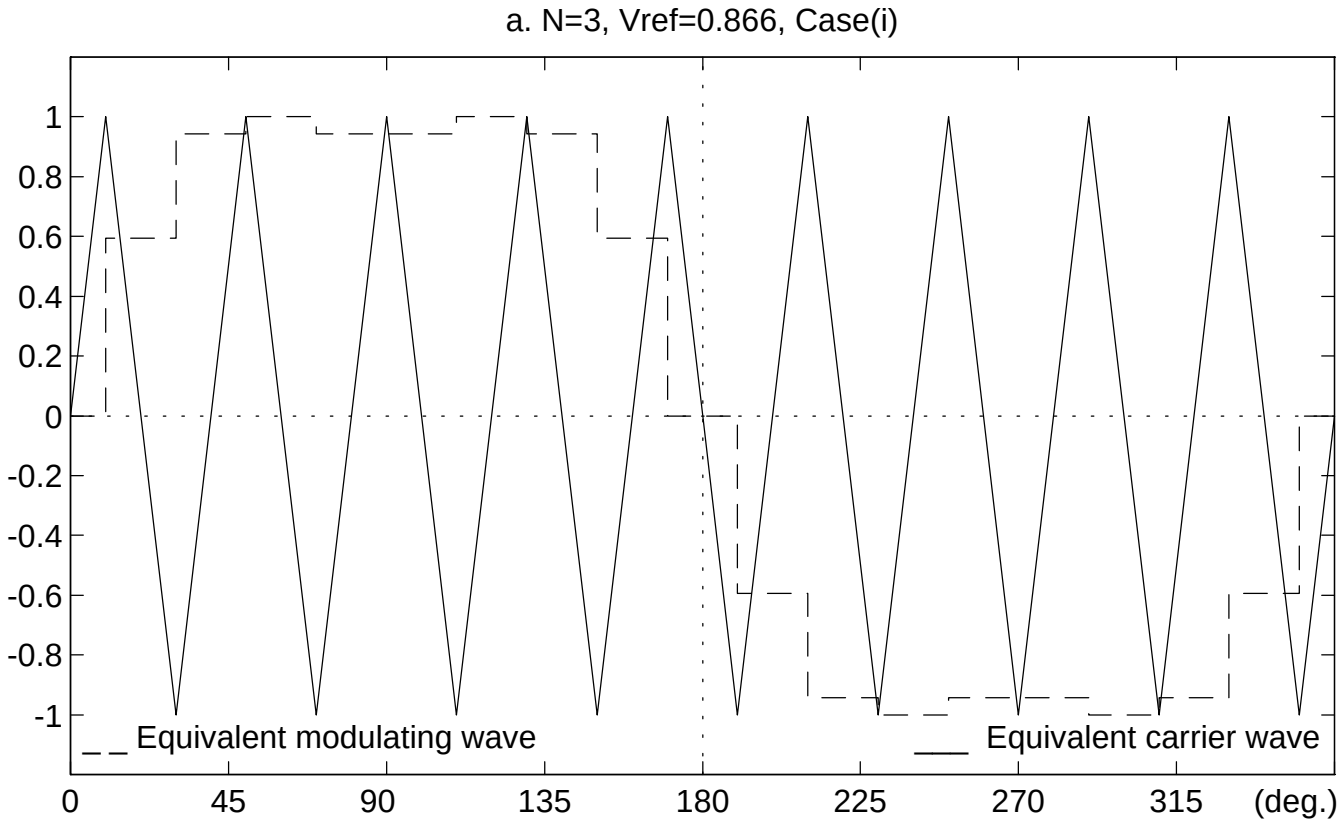

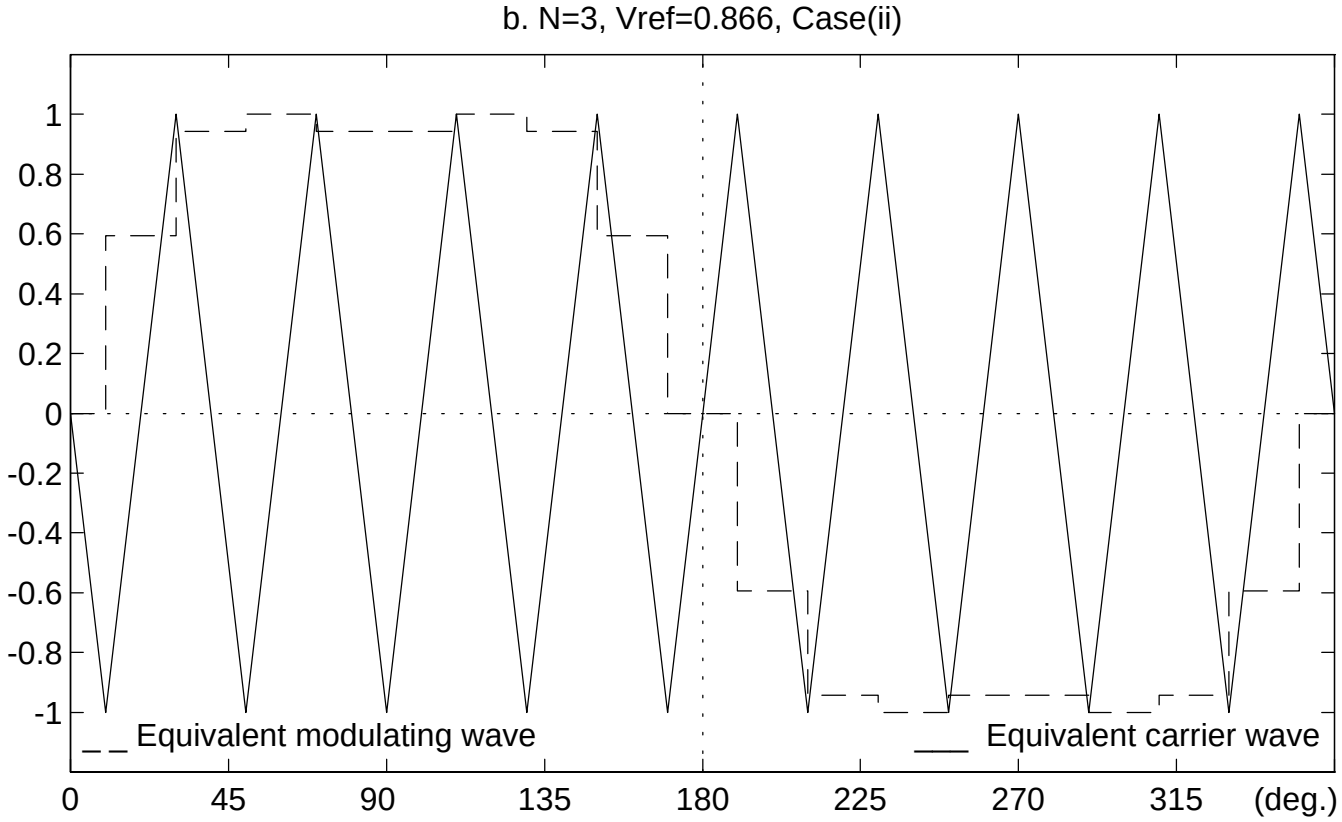

Fig.10 Equivalent modulating and carrier waves - BBCS

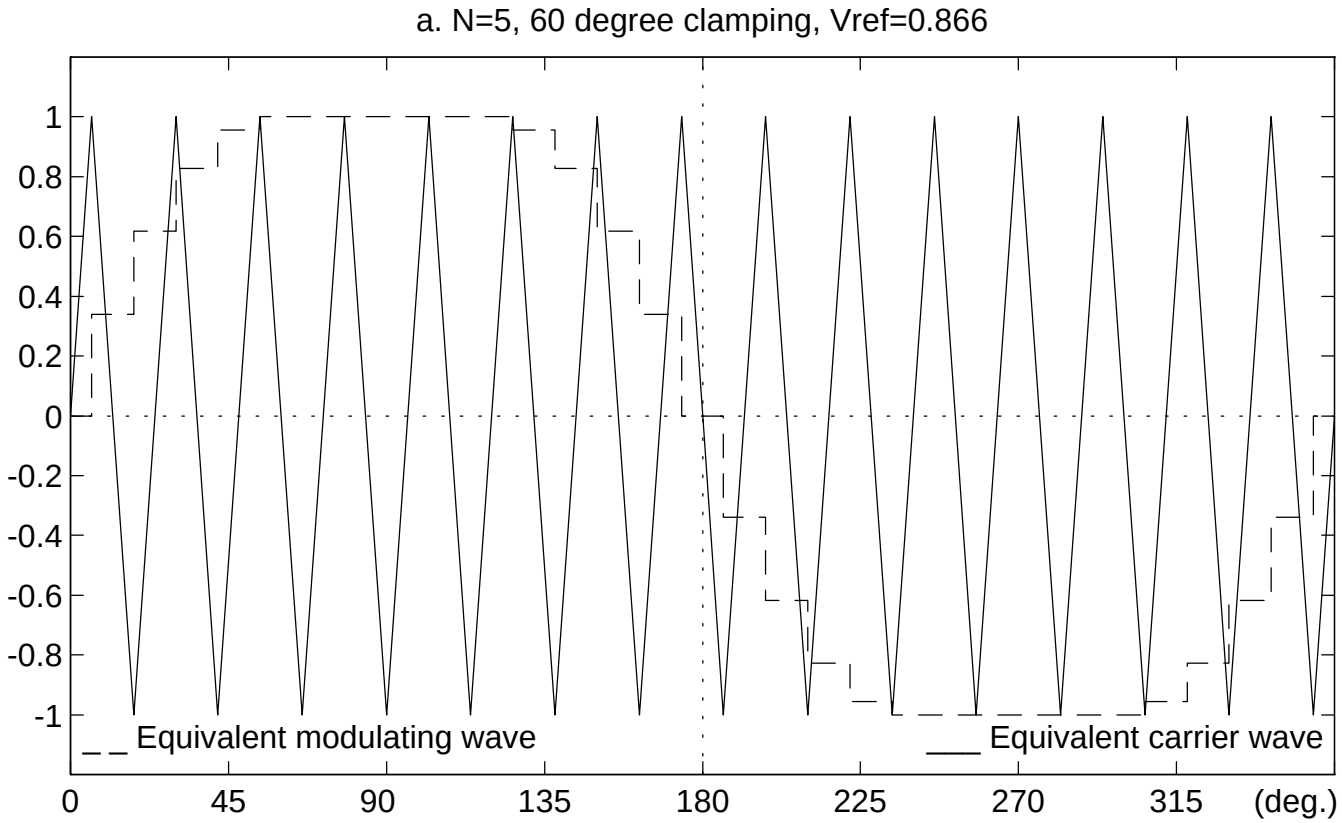

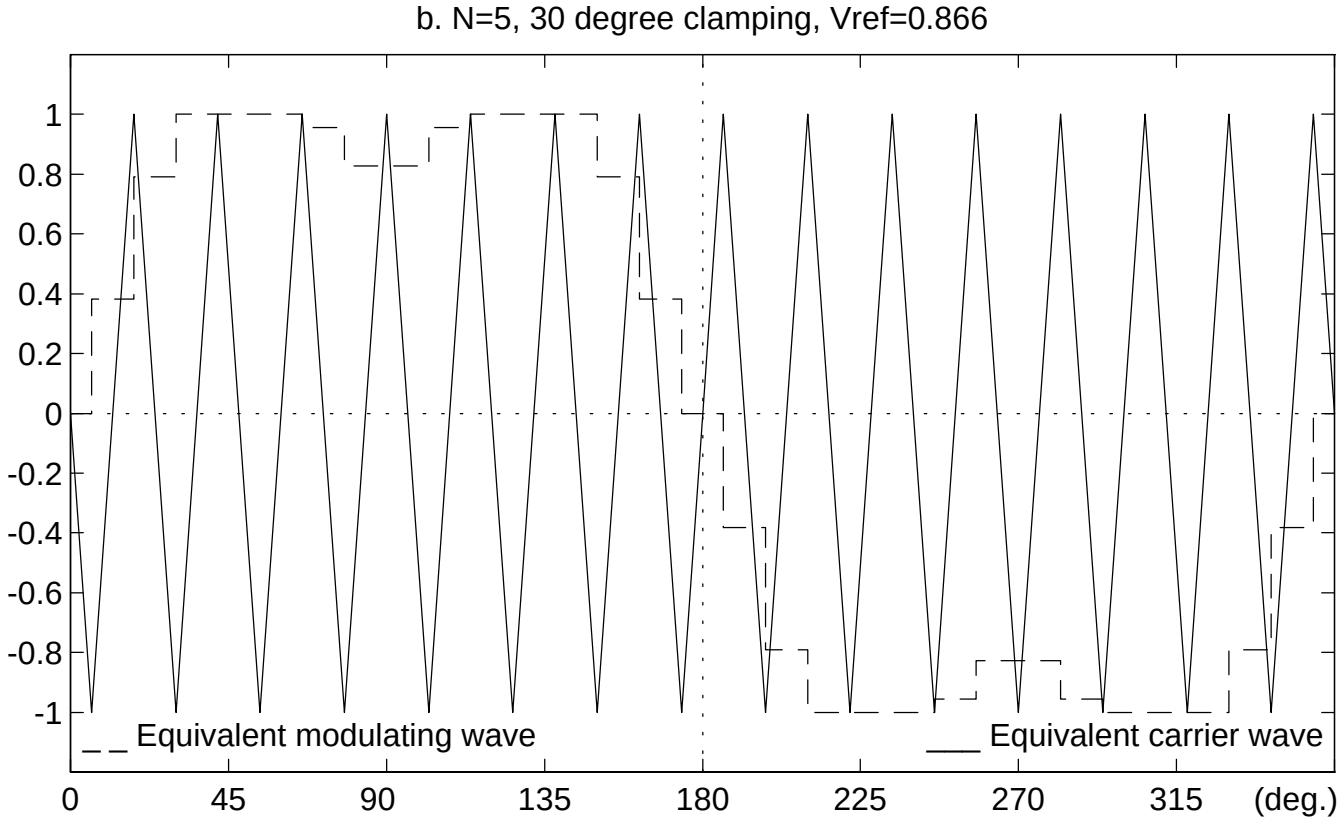

Fig.11 Equivalent modulating and carrier waves of one phase - AZCS

a. N=6, 60 degree clamping, Vref=0.866

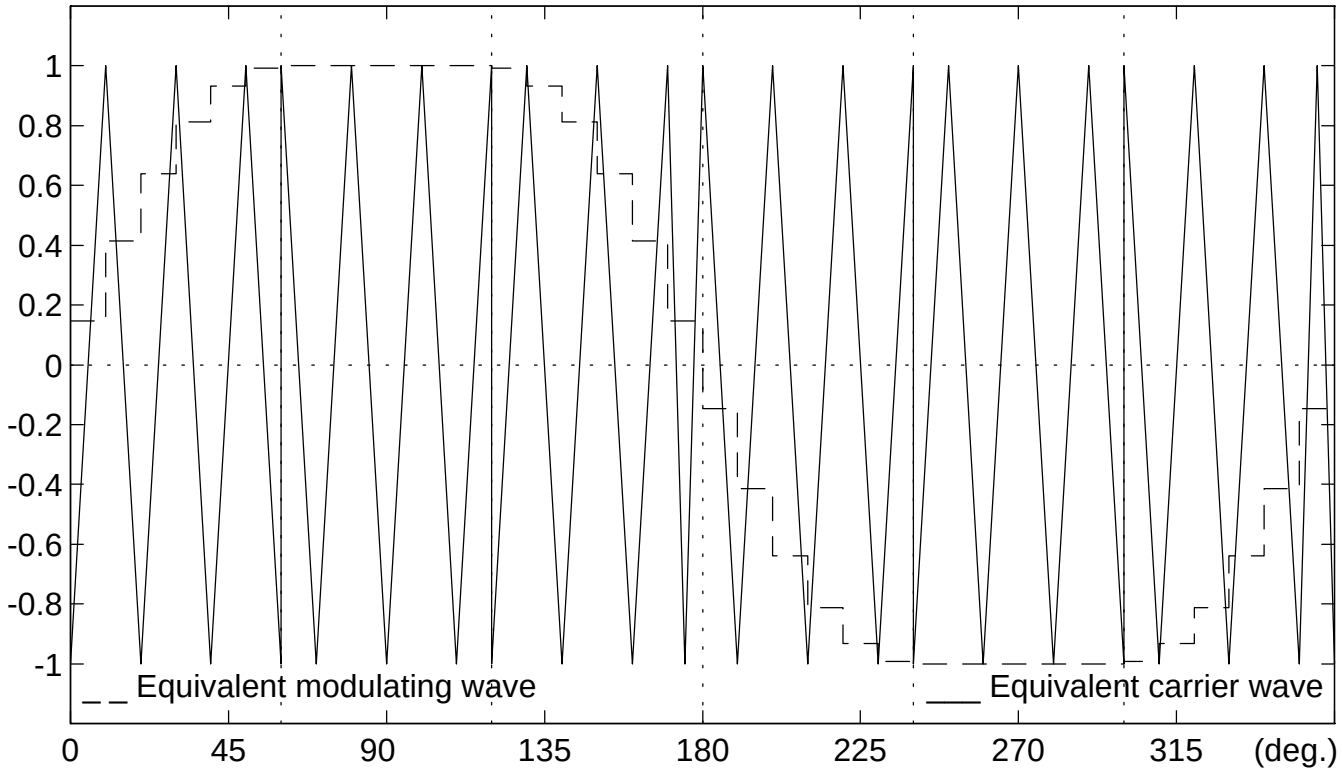

b. N=6, 30 degree clamping, Vref=0.866

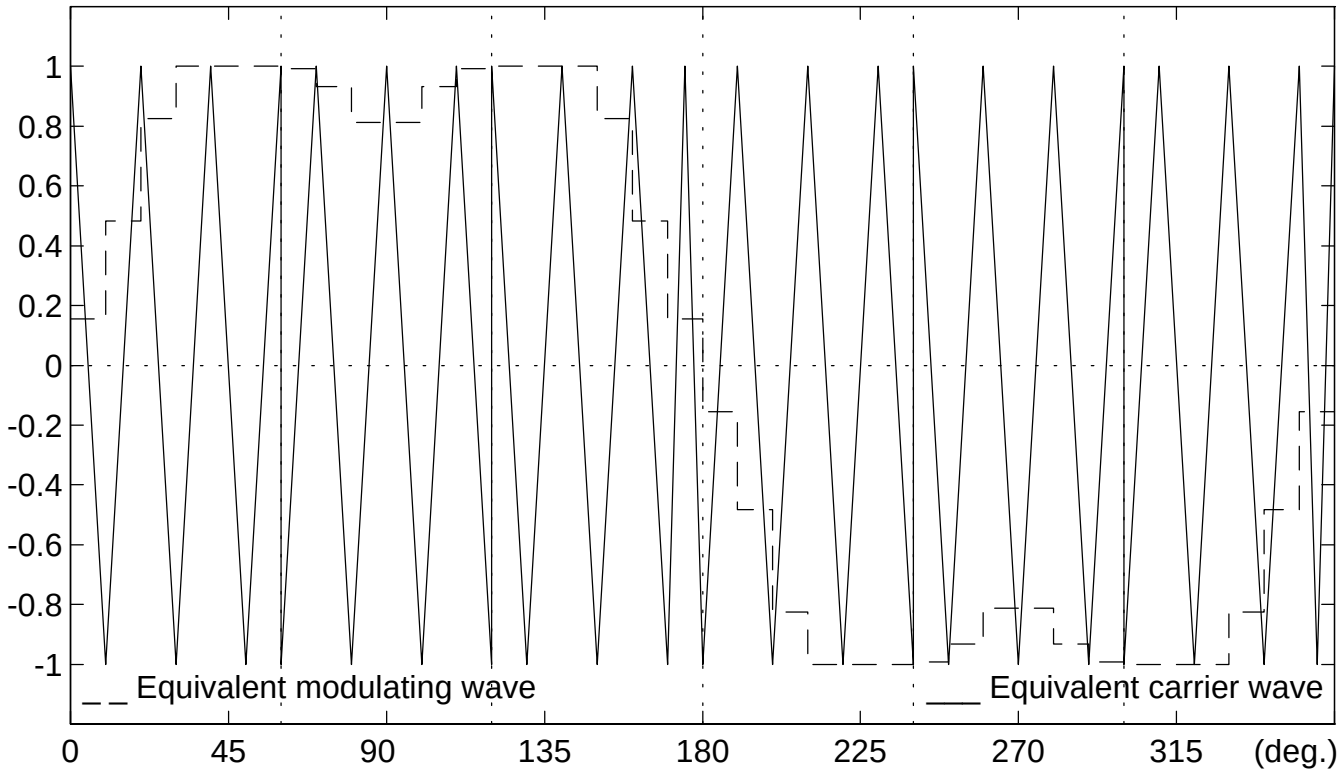

Fig.12 Equivalent modulating and carrier waves of 3 phases - AZCS

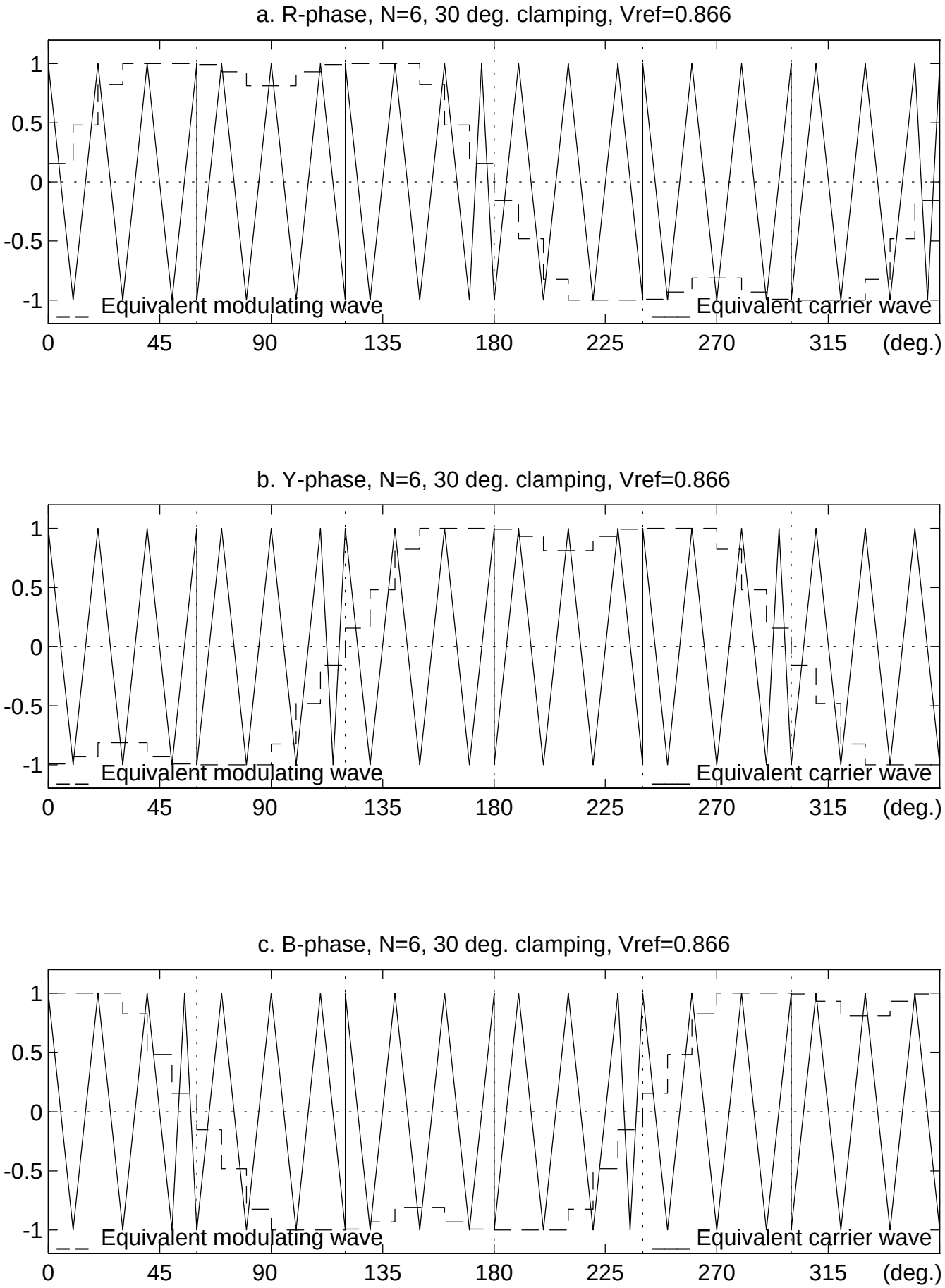

Fig.13 Equivalent modulating and carrier waves - BSS

a. N=4, Vref=0.866

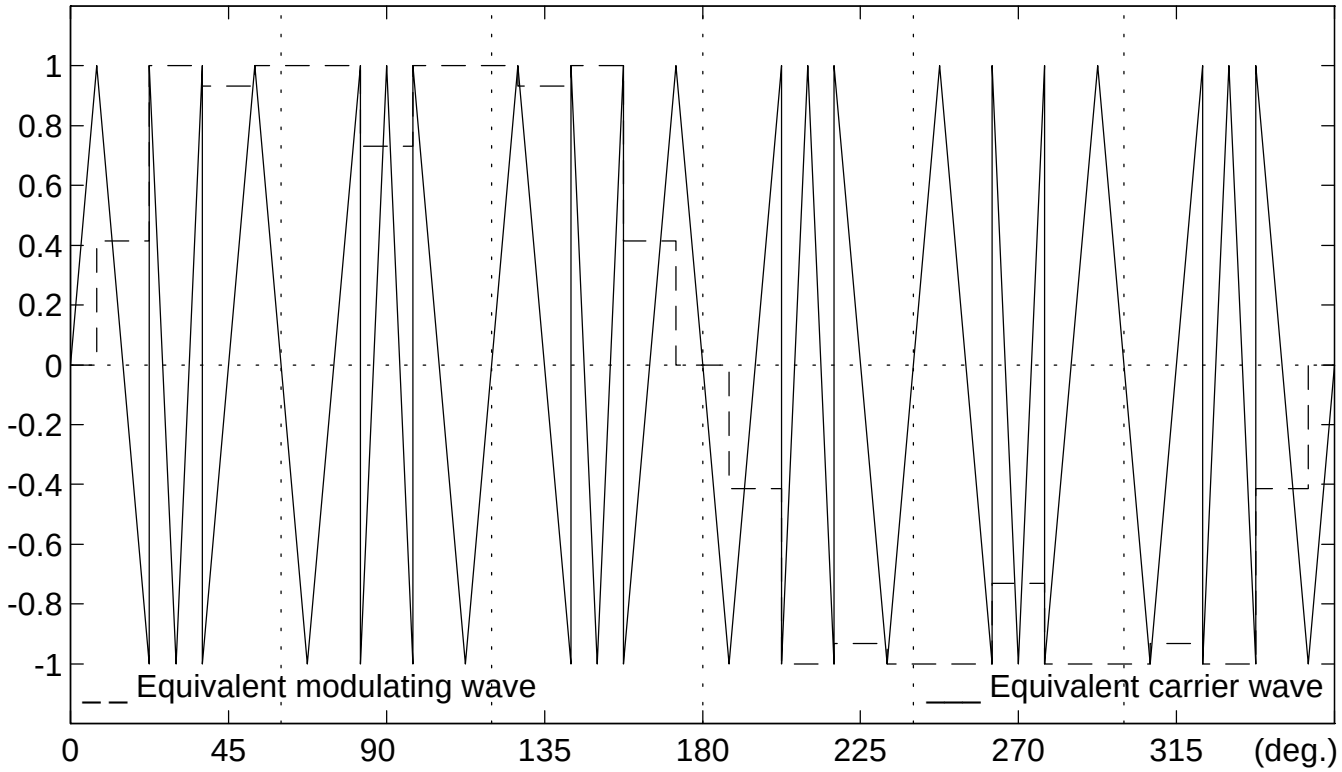

b. N=6, Vref=0.866

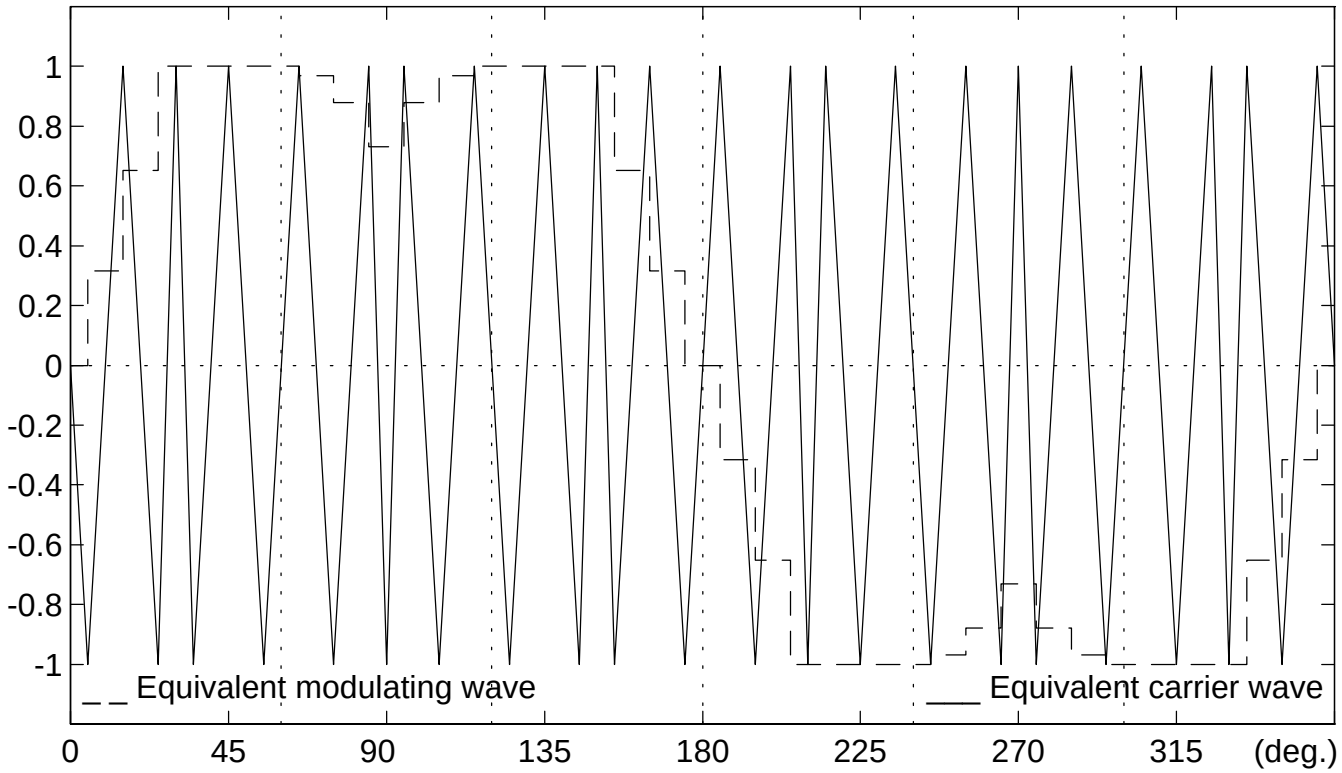

Fig.14 Performance of different strategies for a pulse number of 9

a. Computed Vwthd vs. M characteristics

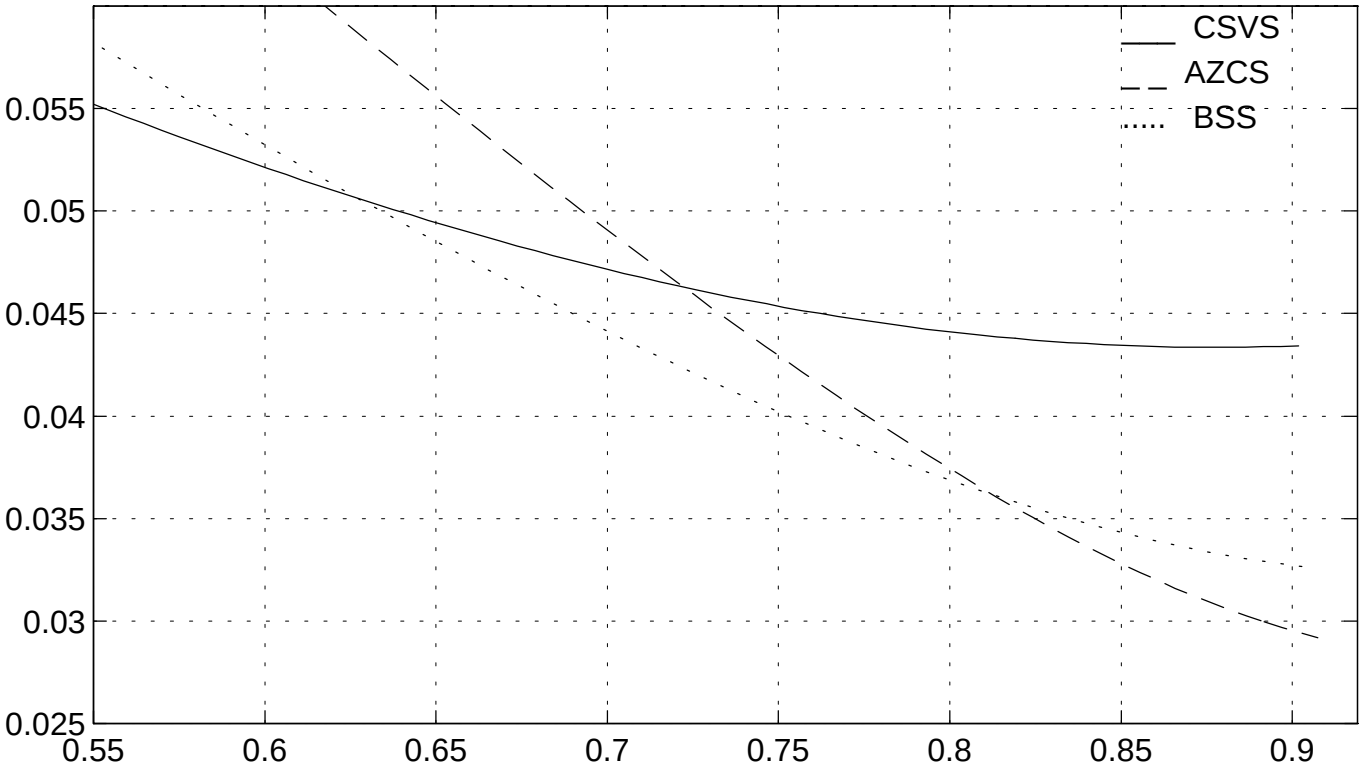

b. Measured Ithd vs. M characteristics